Characteristics of PPG-based Thermoplastic Polyurethane Doped with Lithium Perchlorate

TEN-CHIN WEN,[1] JUI-CHIN FANG,[1] HUNG-JYE LIN,[1] CHIEN-HSIN YANG[2]

[1] Department of Chemical Engineering, National Cheng Kung University, Tainan, 701, Taiwan

[2] Department of Environmental and Chemical Engineering, Kung Shan University of Technology, Tainan, 701, Taiwan

Received 26 May 2000; accepted 15 January 2001

ABSTRACT: Segmented thermoplastic polyurethane (TPU) was synthesized from methylene bis(cyclohexyl isocyanate) (H_{12}MDI), ethylenediamine (EDA), and poly(propylene glycol) (PPG) with a molecular weight of 1000. The ratio of hard segment to soft segment (NCO/OH) is changed to test the chemical and physical properties. Fourier transform infrared spectroscopy (FTIR), differential scanning calorimetry (DSC), and impedance spectroscopy (IS) were utilized to monitor the phase change of these TPU samples with various lithium perchlorate ($LiClO_4$) concentrations. Significant changes occur in the FTIR spectrum of the TPU with $LiClO_4$ concentration above 0.5 mmol/g TPU, indicating that an interaction existed between the lithium cation and the hard segment or soft phase. The soft-segment T_g increased with increasing $LiClO_4$ concentration through the examination of DSC. IS results indicate an increase in bulk conductivity as the salt concentration is increased. Electrochemical stability of the TPU sample was studied by cyclic votammetry (CV). © 2001 John Wiley & Sons, Inc. J Appl Polym Sci 82: 389–399, 2001

Key words: thermoplastic polyurethane; PPG; ionic conductivity; FTIR; electrochemical stability

INTRODUCTION

Pioneering work by Wright et al.[1,2] has inspired a large number of experimental investigations into the properties of polyether–alkali metal salt complexes. Most researchers have concentrated on the design of novel polymer materials possessing high ionic conductivity and mechanical strength, as well as thermal stability, for technological applications.[3–5] The main interest is expected to enhance ionic conductivity; however, morphological studies were also carried out in many applications of solid polymer electrolyte (SPE). Generally, polymer electrolyte is required to exhibit elastomeric property in addition to high ionic conductivity. The dissociation behavior of alkali–metal salts is characterized by the formation of transient crosslinks between ether oxygens in the host polymer and alkali metal cations; the anion is usually not solvated. Ionic transport occurs mainly through a coupling between the ions and polymer segmental motion. To be available in ambient temperature, the polymer–salt electrolyte should be flexible, and applied temperature should be above its glass transition temperature (T_g). On the other hand, solid polymer electrolytes are also necessary to exhibit excellent dimensional stability, having elastomeric properties in their service temperature range.[6]

Correspondence to: T.-C. Wen (tcwen@mail.ncku.edu.tw).

Contract grant sponsor: National Science Council of Republic of China; contract grant number: NSC 89-2214-E006-012.

Journal of Applied Polymer Science, Vol. 82, 389–399 (2001)

Table I Raw Materials for Synthesis of TPU Series

Designation	Chemical Identification	Suppliers
PPG	Polypropylene glycol, M_w = 1000	Showa Chemical Inc. (Tokyo, Japan)
H_{12}MDI	Methylene bis(*p*-cyclohexyl isocyanate)	Aldrich Chemical Inc. (Milwaukee, WI)
DMF	Dimethylformamide	Tedia Company Inc. (Fairfield, OH)
EDA	Ethylenediamine	Merck Chemical Inc. (Darmstadt, Germany)
MeOH	Methyl alcohol	Tedia Company Inc. (Fairfield, OH)
DBTDL	Di-*n*-butyltin (IV) dilaurate	Wako Chemical Co. (Osaka, Japan)

Thermoplastic polyurethanes (TPUs) are composed of a polyether or polyester soft segment and a diisocyanate-based hard segment, which can be characterized by a two-phase morphology.[7] The phase separation due to the fact that the hard and soft phases are immiscible would lead to the formation of a hard-segment domain, soft-segment matrix, and ill-defined interphase. The hard-segment domains act as physical crosslinks and filler particles to the soft-segment matrix and hence are responsible for good mechanical properties of these polymers. The soft-segment domain dissolves most of the salt ions and thus contributes to the conductivity of this complex. The domain formation is derived from the strong intermolecular hydrogen bonding between the hard–hard segments of urethane or urea linkages and hard–soft segments of urethane (or urea) and ether.[8–11] There are some significant parameters, such as the kind of raw materials, the soft-segment molecular weight, and the hard-segment concentration,[12] that could affect the elastomeric properties of TPU.

Infrared spectroscopy was extensively employed to study the hydrogen bondings and was demonstrated as a powerful tool in identifying the characteristics of hydrogen bonding.[9–11,13–24] The hydrogen bonding is characterized by a frequency shift to values lower than those corresponding to the free groups (i.e., no hydrogen bonding). Meanwhile, the extent of the frequency shift is usually used to estimate the H-bonding strength. Particularly polyether-based TPUs, the fraction of the H-bonded carbonyls, is a measure of the hard–hard segment hydrogen bond (NH ··· O═C bond), which was employed to evaluate the extent of phase separation. On the other hand, the fraction of the hydrogen-bonded ether oxygens (NH ··· O bond) represents the extent of phase mixing between hard and soft segments. Recently, several studies have attempted to elucidate the relationships between structure and properties within TPUs by using FTIR[13–24] and DSC.[24–27] Seki et al.[28] and McLennaghan et al.[29,30] have proven that the doped lithium salt of TPUs results in an increase of the soft-segment T_g and a loss of the higher temperature endothermic transitions. More recently, our laboratory[31] has shown that the lithium salt of $LiClO_4$ was observed to increase the overall bulk conductivity of a phase-segregated waterborne polyurethane (WPU) comprising soft segments of poly(propylene glycol) (PPG) and hard segments of isophorone diisocyanate (IPDI) and ethylenediamine (EDA). Significant change occurs in the FTIR spectrum of the WPU when the critical salt concentration is above 1.0 mmol/g WPU, suggesting that an interaction with the lithium cation within the hard segment and between the hard and soft phase occurs. Thus, the characteristic phase-segregated morphology of the WPU has been altered as a result of the interaction of lithium cations within the polar hard domains and by the promotion of phase intermixing due to the coupling of the hard and soft phases. In this study, we will change the ratio of hard segment to soft segment (NCO/OH) for TPU to understand more detailed information about the interaction of lithium cations within the soft and hard segments.

In this work, a PPG-based TPU was synthesized and used as a solid polymer electrolyte. By using FTIR, impedance spectroscopy (IS), and DSC, we investigate the effect of the $LiClO_4$ concentrations on the phase variation, thermal behavior, and bulk impedance properties of a TPU with a composition of H_{12}MDI/PPG/EDA (chain extender).

EXPERIMENTAL

Synthesis of TPU

The raw materials employed in this study are listed in Table I. PPG was dried and degassed in

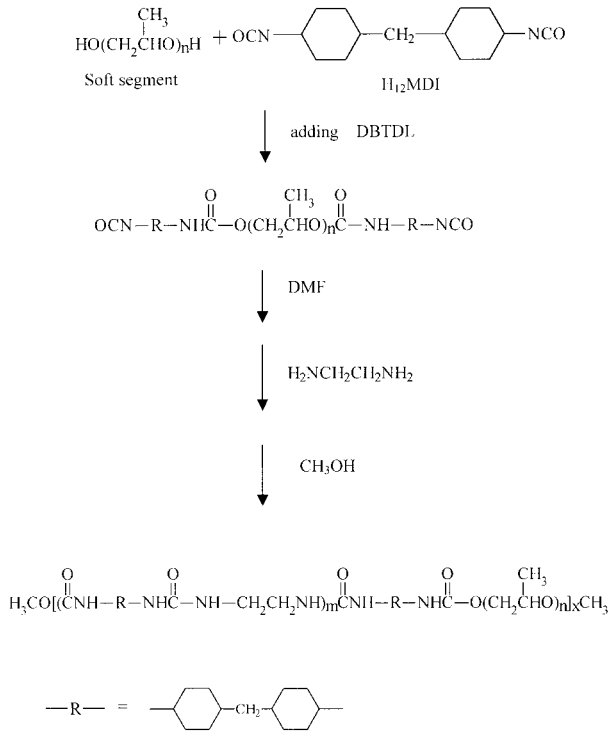

Scheme 1 Outline of the process for preparing TPU.

the vacuum oven under 85°C for 1 day. All other chemicals were used without further treatment. An outline of the process used in this study for preparation of PPG-based TPU solution is shown in Scheme 1. The TPU(PPG) prepolymer was synthesized by a one-step addition reaction in a 2-L four-necked round-bottomed flask completed with an anchor-propeller stirrer, a nitrogen inlet and outlet, and a thermocouple connected to the temperature controller.

PPG (100 g, 0.1 mol) and methylene bis(cyclohexyl isocyanate) ($H_{12}MDI$) (81.33 g, 0.31 mol for hard/soft ratio 3 : 1 or 55.09 g, 0.21 mol for hard/soft ratio 2 : 1) were simultaneously added to the reactor under a nitrogen gas atmosphere to make the prepolymer of TPU where the ratio of NCO/OH is 3 or 2. The temperature was kept at 50°C initially. After proper mixing (150 rpm), two drops of dibutyltin dilaurat (DBTDL) was added into the batch to catalyze the reaction and then the temperature of the batch was increased to 85°C. After 6 h reaction at this temperature, 1000 g dimethylformamide (DMF) was added to dissolve the prepolymer completely. Then the chain extender, EDA (12.6 g, 0.21 mol or 6.6 g, 0.11 mol, as the case may be), which was previously diluted to a 10% solution in DMF, was added slowly to convert the prepolymers into polymers. Viscosity was increased in this step. After a half-hour reaction, a few drops of methyl alcohol (MeOH) were added to terminate the reaction.

Molecular Weight

The number-average molecular weight (M_n) and weight-average molecular weight (M_w) were determined by use of a Shimadzu GPC fitted with a Shimadzu HPLC pump and a differential refractometer. A Jordi gel DVB mixed-bed 250 $\times$ 10-mm column was employed for the analysis. DMF was used as the continuous phase and was pumped through the column at a flow rate of 2.0 mL/min. This system was calibrated against 10 polystyrene standards. The measured molecular weight distribution of the synthesized TPUs are shown in Table II.

Preparation of Polymer Film

Lithium perchlorate ($LiClO_4$) was dissolved into DMF to make 10 wt % $LiClO_4$/DMF solution. TPU solutions (ca. 10 wt %) were blended with different amounts of 10 wt % $LiClO_4$/DMF solution to incorporate different concentrations of $LiClO_4$ in the TPU system. The blended solutions were poured into a glass dish to make the desired lithium salt-doped polymer films. The solution was dried in a vacuum oven for 3 days at 50°C. Four different concentrations of $LiClO_4$ were chosen in each type of TPU, 0.0, 0.5, 1.0, and 1.5 mmol $LiClO_4$/g TPU. In this study, the polymer electrolytes with three for the NCO/OH ratio in addition to electrolyte concentrations 0.0, 0.5, 1.0, and 1.5 mmol $LiClO_4$/g TPU are assigned samples f1, f2, f3, and f4, respectively, whereas those with two for the NCO/OH ratio are denoted as g1, g2, g3, and g4 for 0.0, 0.5, 1.0, and 1.5 mmol $LiClO_4$/g TPU, respectively.

After drying, the films were transferred into a glove box in a vacuum chamber for further drying. Before all tests of these films, the water content of these films was determined to be around 10 ppm

Table II Molecular Weights and the Distributions of the Synthesized TPU Series

Molecular Weight	TPU3	TPU2
M_n	106,000	74,000
M_w	237,000	238,000
PDI (M_w/M_n)	2.236	3.216

by Karl Fisher moisture titrator (Model 275KF, Denver Instrument, USA).

Fourier-Transform Infrared Spectroscopy

Films for FT infrared analysis were prepared by casting films for a 2% DMF solution onto potassium bromide windows at room temperature. Following evaporation of the majority of the solvent, the films were placed in a vacuum oven at about 80°C for over 24 h to remove residual solvent and moisture.

FTIR spectra were collected by using a Nicolet 550 system at a resolution of 2 cm^{-1}, and a minimum of 64 scans were signal-averaged at room temperature. Band deconvolution of the resulting spectra was obtained by analysis with Grams 386 software (Galactic). The maximum error associated with the deconvolution of the IR spectra is expected to be ±5%. In most cases, the deconvolution was executed by fitting the spectra to different functions to assure the accuracy of the deconvolution results.

DSC Thermograms

Thermal analysis of TPU was carried out by using DSC (TA DSC 2010, USA). The temperature was equilibrated first at −100°C and then scanned from −100°C to +100°C at a heating rate of 10°C/min. Samples were taken from TPU film and sealed in aluminum capsules and transferred out of a dry box to perform thermal analysis.

Impedance Spectroscopy

Impedance measurements were performed in the cast films of about 150–200 μm thickness and 0.785 cm^2 area. The ionic conductivity of the TPU films sandwiched between two stainless steel electrodes was measured by using Autolab PGSTAT 30 equipment (Eco Chemie B.V., Netherlands) with the help of the Frequency Response Analysis system software under an oscillation potential of 10 MV from 100 to 1 kHz. Then the conductivity was calculated by using the relation $\sigma = (1/R_b) \times (l/A)$, where R_b is the bulk resistance from AC impedance, l is the film thickness, and A is the surface area of electrode.

Cyclic Voltammetry

Three electrode-laminated cells were assembled inside a glove box for cyclic voltammetry experiments. Lithium metal was used as a counter as well as a reference electrode and stainless steel (SS) was used as a working electrode. Cyclic voltammetric measurements were carried out by using Autolab PGSTAT 30 potentiostat/galvanostat equipment (Eco Chemie B.V., Netherlands).

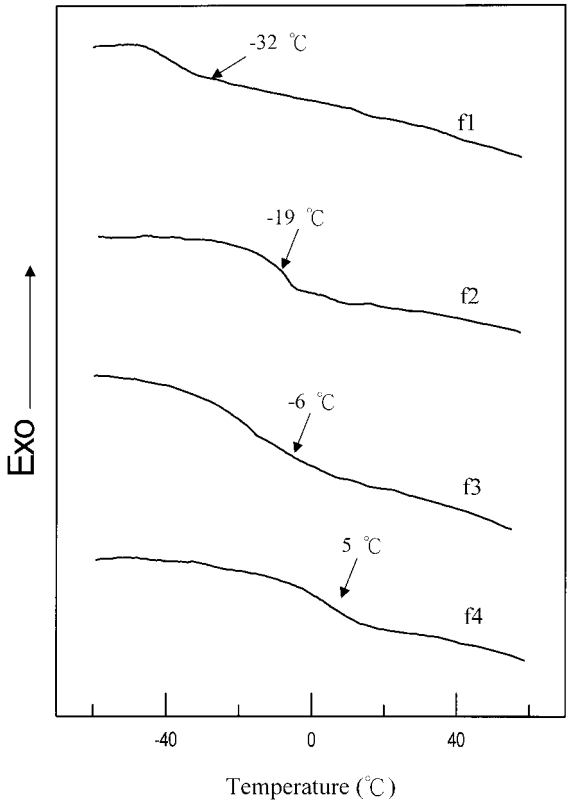

Figure 1 DSC thermograms for the TPU3 series doped with various $LiClO_4$ concentrations: (f1) 0, (f2) 0.5, (f3) 1.0, (f4) 1.5 mmol/g TPU.

RESULTS AND DISCUSSION

DSC

DSC was utilized to examine the effect of $LiClO_4$ on the polyether soft-segment T_g of the TPU. Figure 1 shows the DSC thermograms of TPU3 (NCO/OH = 3) and TPU3–$LiClO_4$ complexes with various $LiClO_4$ concentrations. An examination of Figure 1 reveals that the T_g of the PPG soft segment is increased by increasing the salt concentration. The results of the DSC analysis are summarized in Table III. In salt-free TPU3 (f1 sample), the T_g of the soft segment appeared at −32°C. With increasing $LiClO_4$ concentration from 0 to 1.5 mmol/g TPU, T_g of the soft segment is increased to 5°C. This result reflects the finding

Table III Thermal Properties of TPU(PPG) and TPU(PPG)-$LiClO_4$ Complexes

Film Number	mmol [$LiClO_4$]/g TPU (PPG1000)	T_g (range) (°C)	ΔT_g [a] (°C)	Increase in T_g (°C)
		Hard/soft = 3 (TPU3)		
f1	0	−32 (−39 to −30)	9	
f2	0.5	−19 (−27 to −11)	16	13
f3	1.0	−6 (−11 to −5)	6	26
f4	1.5	5 (2 to 7)	5	37
		Hard/soft = 2 (TPU2)		
g1	0	−37 (−44 to −33)	11	
g2	0.5	−17 (−23 to −13)	10	20
g3	1.0	−6 (−13 to −2)	11	31
g4	1.5	2 (−5 to 12)	17	39

[a] ΔT_g represents the range of T_g variation.

that the solvation of the lithium cation by the PPO soft segment partially arrests the local motion of the polymer segment through the formation of transient crosslinks, leading to an increase in the soft-segment T_g. Moacanin and Cuddihy[32] reported that the T_g of the PPO soft segment increased considerably with increasing $LiClO_4$ concentration. They interpreted the increase in T_g by assuming a copolymer of complexed propylene oxide (PO) unit with $LiClO_4$ and pure PO units generate as $LiClO_4$ dissolved into PPO units. An increase in T_g is due to a change in the copolymer composition with increasing $LiClO_4$ concentration. Thus, the increase in T_g of the soft segment in the present system provides evidence that $LiClO_4$ is selectively dissolved in the PPO phase. The glass transition zone (ΔT_g) had a maximum at a $LiClO_4$ concentration of 0.5 mmol/g TPU. Complexed PO units may be located randomly by $LiClO_4$ along the soft segment.[26] The superposition of the behavior of the free and complexed PO units may result in the wider distribution of the relaxation times. This phenomenon results in a large glass transition zone. At higher $LiClO_4$ concentration, most PO units are almost complexed with $LiClO_4$, leading to the distribution of the relaxation times becoming narrow again.

The T_g of the soft segment of salt-free TPU2 (NCO/OH = 2) (g1 sample) was −37°C, which was lower than that of TPU3 (f1 sample). The reason is that soft-segment domain ratio of TPU2 is more than that of TPU3. With increasing $LiClO_4$ concentration, the T_g increase of the soft segment is similar to the behavior observed in the TPU3 series. It is obvious that the T_g's in the TPU2 series were somewhat lower than that in the TPU3 series at same $LiClO_4$ concentration. This is ascribable to TPU2 containing more soft segment, which consumes less energy to initiate the motion of soft segment.

Fourier Transform Infrared Analysis

FTIR was utilized at ambient temperature (25°C) to study the effect of salt concentration on the phase morphology of the TPU. In this work, the stretching vibration in the range of 3200–3650 cm^{-1} is mainly an interested interval. To directly study the extent and strength of hydrogen bondings in both hard–hard and hard–soft segments, the experiments were performed by varying the salt concentration.

NH Stretching Region

Figure 2 shows the IR spectra of the NH stretching region with doping various salt concentrations ranging from 0 to 1.5 mmol $LiClO_4$/g TPU. In each spectrum, the NH stretching vibration exhibits a strong absorption peak centered at around 3330–3370 cm^{-1}, arising from the hydrogen bonding between N—H and carbonyl groups, whereas the free NH stretching vibration appears at ca. 3500–3503 cm^{-1}. Note that there appears another obvious shoulder or peak at ca. 3280–3310 cm^{-1}. This peak corresponds to the NH $\cdots$ O hydrogen bonding which is established on the basis of the previously evidenced existence of the NH stretching vibration at ca. 3258–3295 cm^{-1}.[18] This result is attributable to the phase-mixed state between hard and soft segments via hydrogen bonding in the polymers.

Deconvolution of the NH stretching region was found to be the best fits by using a Gaussian–

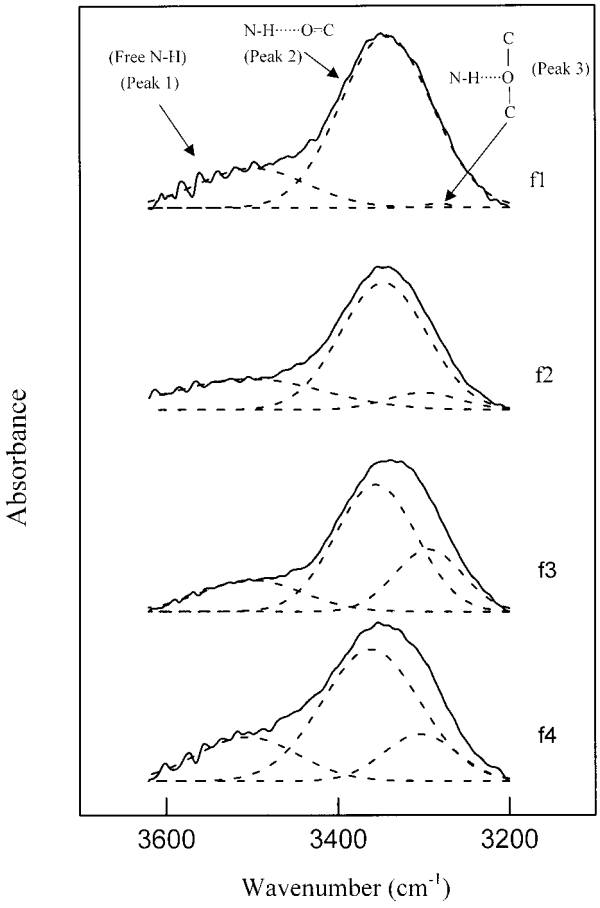

Figure 2 The decomposition of N—H stretching for TPU3 doped with various $LiClO_4$ concentrations: (f1) 0, (f2) 0.5, (f3) 1.0, (f4) 1.5 mmol/g TPU.

Lorentzian sum. The maximum frequency (ν) and area of each band were determined by using the Nelder–Mead optimization method. As shown previously by many researchers,[17,18] the typical free NH band at ca. 3440 cm^{-1} appears as a low-intensity shoulder on the measured TPUs. The free NH stretching vibration of peak 1 is enhanced due to the increase in salt concentration. All NH band areas were normalized on the basis of total N—H stretching band area and are listed in Table IV. Band shift of free NH stretching for both the TPU3 and the TPU2 is approximately proportional to salt concentration, but the band area of those samples is not changed with various salt concentrations. The band shift in this work is presumably due to the interaction between the Li^+ cation and the lone pair of electrons on the nitrogen atom,[31,33] leading N—H bond length to be reduced as follows:

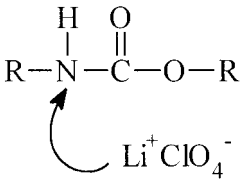

For TPU3 samples, the band of hydrogen bonding between NH and carbonyl (peak 2) was shifted from 3344 cm^{-1} for the f1 sample (0 mmol $LiClO_4$/g TPU) to 3362 cm^{-1} for f4 sample (1.5 mmol $LiClO_4$/g TPU). Because band position is related to the strength of the H-bonded NH band, the shift to higher frequency with increasing salt concentration indicated an increase in the bond strength of the N—H bond. This is likely due to the localization of the electron-rich oxygens through coordination of the Li^+ cation with the hydrogen-bonded species:

Table IV Deconvolution Results of the N—H Stretching Region for TPU(PPG) and TPU(PPG)-$LiClO_4$ Complexes

TPU Film Number	Peak Position (cm^{-1})			Peak Area (%)[a]		
	Peak 1	Peak 2	Peak 3	Peak 1	Peak 2	Peak 3
f1[b]	3500	3344	3283	21	78	1
f2	3500	3350	3289	20	69	11
f3	3501	3356	3294	18	58	24
f4	3503	3362	3304	20	62	18
g1	3501	3345	3284	21	70	9
g2	3502	3347	3293	21	67	12
g3	3501	3352	3296	20	58	22
g4	3503	3352	3306	20	57	23

[a] The band areas are based on total N—H stretching area.
[b] f1, g1: 0 mmol/g TPU. f2, g2: 0.5 mmol/g TPU. f3, g3: 1.0 mmol/g TPU. f4, g4: 1.5 mmol/g TPU.

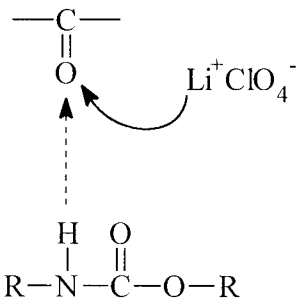

Thus, the strength of the hydrogen bonding between NH and carbonyl is weakened, resulting in the shift to higher frequency for the NH band affected by carbonyls. As well, the band area (peak 2) decreased with increasing the salt concentration as shown in Table IV. This result provides evidence that the possibility of the hydrogen bonding between NH and carbonyl is decreased. Similarly, the above phenomena also appear in TPU2 films.

In Table IV, it is clear that the band position of NH stretch for H-bonding to either the carbonyl or the ether oxygen (peaks 2 and 3, respectively) shows almost no change with the hard/soft ratio at the same concentration of salt. On the other hand, the band area of peak 2 decreases with increasing in hard/soft ratio, but that of peak 3 increases. This phenomenon is reasonable in the sense that the same environment of the NH group occurs with change in the hard/soft ratio and that the density of NH groups for H-bonding to either carbonyl (hard segment) or ether (soft segment) oxygen changes with the change in the hard/soft ratio. Hence, the band position for both peaks (peaks 2 and 3) does not vary with the hard/soft ratio. The availability of carbonyl or ether oxygen varies with the change in the hard/soft ratio and hence the area is also varied. In TPU3 samples, the hard segment proportion is higher than that in TPU2 samples, leading to a higher area of peak 2 (which corresponds to NH stretching for hydrogen bonded to carbonyl oxygen of the hard segment) in comparison to TPU2 samples. Similarly, the proportion of soft segment in TPU3 samples is less than that in TPU2 samples. Thus, the area of peak 3 (which is assigned to NH stretching for H-bonding to ether oxygen of the soft segment) for TPU3 samples is lower than that for TPU2 samples.

It is worth noting that the variation of the peak area for peaks 2 and 3 is related to $LiClO_4$ concentration. For both TPU samples, the area of peak 3 increases with increasing $LiClO_4$ concentration (refer to Table IV); the converse is true for peak 2. One possible explanation for this phenomenon may be that more and more ether oxygens would be coordinated by Li^+ ions with increasing salt concentration. Owing to the inductive effect of the coordinated Li^+ ions, more NH groups would be H-bonded to ether oxygens. This situation can be illustrated by the following expression:

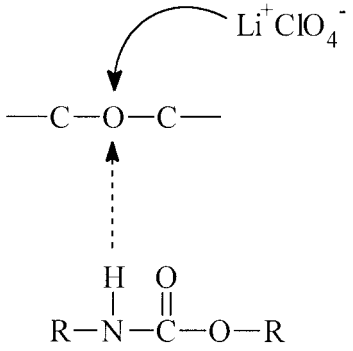

Thus, the area of NH peak hydrogen bonded to the soft segment (peak 3) increases with increasing salt concentration. In contrast, the area of peak 2 decreases with increasing salt concentration in Table IV. This result provides evidence that the possibility of the H-bonding between N—H and carbonyls is decreased.

Conductivity Analysis

It is very interesting to investigate the conductivity of TPU-based electrolytes. Figures 3 and 4 illustrate the temperature dependence of ionic conductivity for the TPU3–$LiClO_4$ complexes and TPU2–$LiClO_4$ complexes, respectively. From an examination of these figures, there exists evidence that the bulk conductivity insignificantly increases with the increase in the doped salt concentration. Similar to that observed by McLennaghan et al.,[30] a maximum conductivity is observed as a function of concentration over the entire temperature range. There is an obvious transition at 55°C in Figures 3 and 4, respectively. In Figure 3, the conductivity of the f2 sample is higher than that of f3 and f4 samples at below 55°C. In contrast, the conductivity of the f2 sample is lower than that of other two films at above 55°C. This result may be explained by the finding that ions are predominantly coupled to the segmental motions of the host polymer at below 55°C and the phenomena will change at temperatures above 55°C. It might be attributed

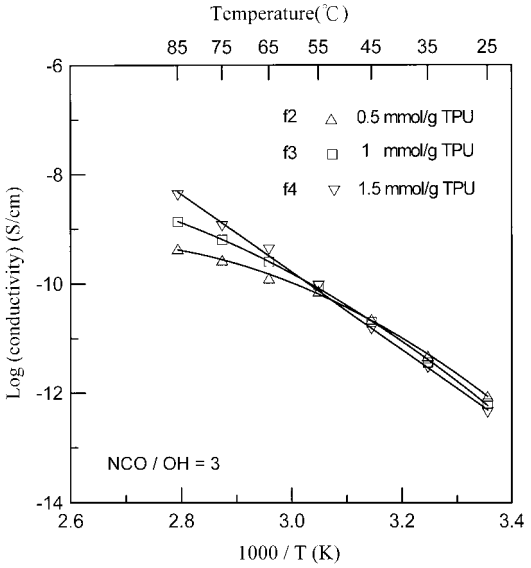

Figure 3 Temperature dependence of conductivity for TPU3–$LiClO_4$ complexes.

to the mobility effect. Above 55°C, the conductivity is determined by doped various salt concentrations. In the temperature range of this case, it is obvious that the order of the conductivity is f4 > f3 > f2. This might be due to the concentration effect.

In Figure 4, it is also obvious that the conductivity of the g2 sample is higher than that of g3 and g4 samples at below 55°C. In contrast, the conductivity of the g2 sample is lower than that of other two films at above 55°C. This is almost similar to the result of Figure 3. However, there still exists a discrepancy between the two figures, being that the results of g2 and g3 samples stay linear.

In Figure 3, the result of the f2 sample exhibited a curved line. This result can be explained by the finding that the ratio of salt dissolved in the TPU3 soft segment is obviously less. Therefore, the increase in conductivity becomes alleviative; the effect of temperature becomes insignificant. This result also can be supported by DSC examination. This is attributable to the existence of coordination between $LiClO_4$ salt and soft segment of TPU. In Table III, the change of T_g between f1 and f2 samples is 13°C, which is less than that (20°C) between g1 and g2 samples. This reflects the finding that the salt quantity of soft segment doped in the f2 sample is less than that of g2 sample; hence, the tendency of conductivity in this temperature range exhibits the alleviative trend. On the other hand, the change of T_g between the f1 and f4 samples is similar to that between the g1 and g4 samples. This leads to the same linear results in the f4 and g4 samples.

In Table IV, the difference in peak 3 between the f1 and f2 samples is larger than that between g1 and g2 samples. This is likely due to the localization of the electron-rich oxygens through coordination of Li^+ cation with H-bonding species. Thus, the strength of the hydrogen bonding between NH and carbonyls is weakened. The shift of peak 3 is more obvious. This implies that the effect of $LiClO_4$ salt concentration becomes significant. At the same doping salt concentration, the doping of $LiClO_4$ salt in soft segment for TPU2 is more than that for TPU3. Thus, the conductivity of TPU2 series is higher than that of TPU3 series.

To improve the conductivity, TPU2 and TPU3 series, respectively, were impregnated with PC to form gel-type electrolytes. Figure 5 shows the PC intaking content as a function of intaking time for the TPU–$LiClO_4$ complexes. In Figure 5(a), the result of f1 sample showed a rubbery plateau level of 15% over a wide time range (100–300 s). This indicates the typical characteristics of TPU which could not intake PC very much. When $LiClO_4$ was doped in the TPU3, the PC intaking content increases with increasing salt concentration, indicating that the increase in intaking content of PC is enhanced by salt concentration.

Figure 5(b) shows the PC intaking content as a function of time for the TPU2–$LiClO_4$ complexes.

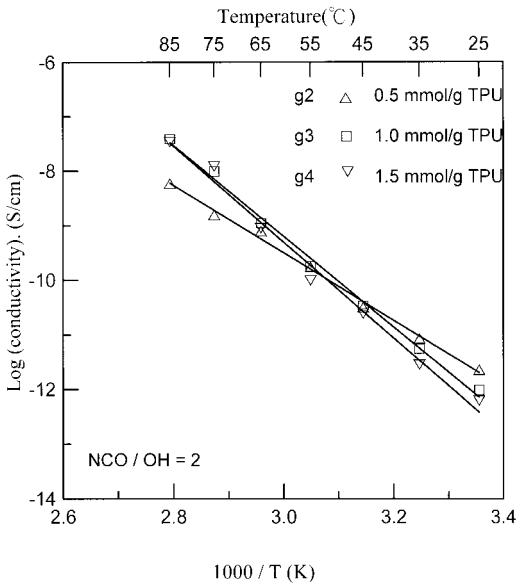

Figure 4 Temperature dependence of conductivity for TPU2–$LiClO_4$ complexes.

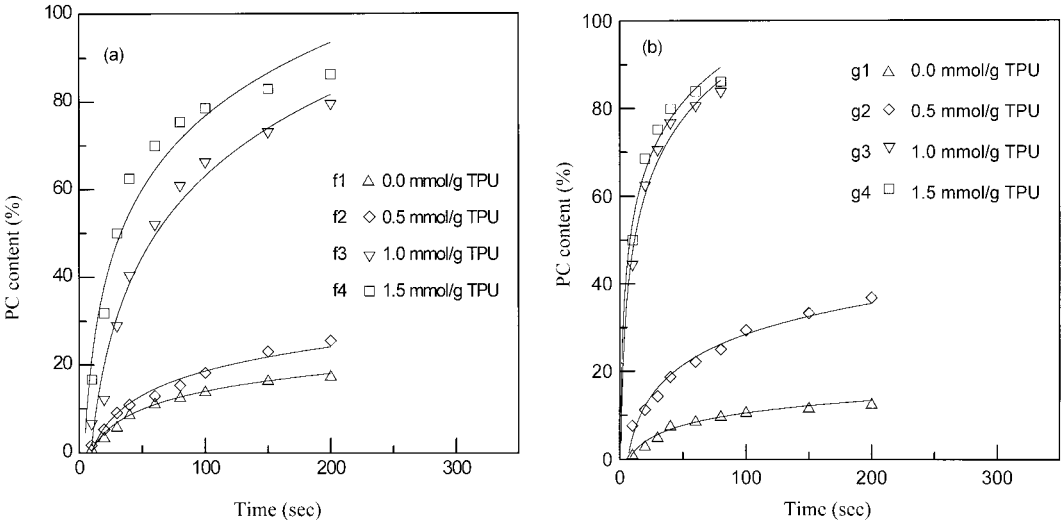

Figure 5 PC content against time for (a) TPU3–$LiClO_4$ complexes and (b) TPU2–$LiClO_4$ complexes.

In comparison to Figure 5(a), the swelling rate of the TPU2 series is larger than that of TPU3 series. This situation arises from TPU3 series possessing more urethane groups that result in more H-bonding between hard segments to retard PC absorption. Also note that PC is mainly absorbed in the soft segment of PPG. On the other hand, the soft segment of TPU2 series yields more $LiClO_4$ salt. Thus, the swelling rate of TPU2 series is faster than that of TPU3 series.

To understand the characteristics of TPU gel-type electrolytes, we added ca. 50% PC as a plasticizer into the abovementioned TPU samples and then measured the temperature dependence of the conductivity. The lithium ions are decoupled from the polymer host and activated hopping is required for ionic transport after PC addition. Thus, the Arrhenius equation is used to describe this conductivity behavior. Figure 6 shows the Arrhenius plot of ionic conductivity

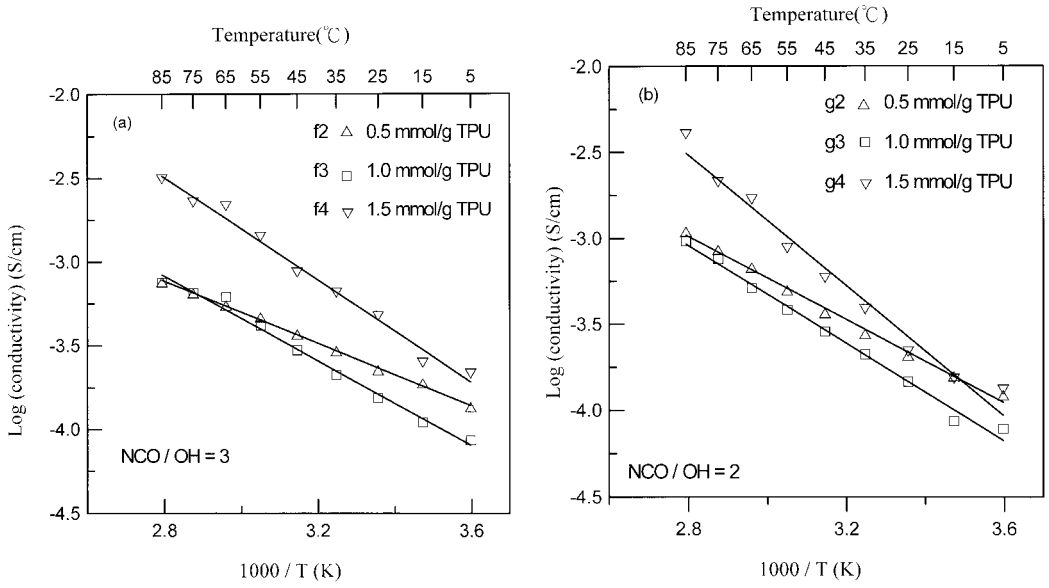

Figure 6 Arrhenius plots of conductivity for (a) various TPU3–$LiClO_4$ complexes containing 50% PC; (b) various TPU2–$LiClO_4$ complexes containing 50% PC.

for the TPU/$LiClO_4$ complex with the addition of 50% PC.

The temperature dependence of conductivity for TPU3/$LiClO_4$ samples with 50% PC is shown in Figure 6(a). The conductivity is significantly increased with the addition of PC in TPU3 than with Figure 3. This result suggests that the intermolecular H-bonding is decreased in these TPU3 samples, leading to a larger transport space of charge carriers (lithium ions). The magnitude of conductivity is in the order f4 > f2 > f3 samples. The temperature dependence of conductivity for TPU2/$LiClO_4$ samples with 50% PC is shown in Figure 6(b). The conductivity is also significantly increased with the addition of PC in TPU2 than with Figure 4. This interpretation is the same as that of TPU3/$LiClO_4$ results. The magnitude of conductivity is in the order g4 > g2 > g3 samples. In both TPU/$LiClO_4$ cases, there exists a similar tendency of ionic conductivity when PC was added into these TPU complexes because the solvation of the lithium cation by the PPO soft segment partially arrests the local motion of polymer segment through the formation of transient crosslinks. At a salt doping level of 0.5 mmol $LiClO_4$/g TPU (f2 and g2 samples), these transient crosslinks are less significant than that of the 1.0 mmol $LiClO_4$/g TPU doping level (f3 and g3 samples), leading to a higher conductivity for the f2 (or g2) sample. On the other hand, there exists the highest conductivity among the three samples when the doping salt is further increased to 1.5 mmol $LiClO_4$/g TPU (f4 and g4 samples). This result is attributable to the existence of excess free $LiClO_4$ salt. This excess free $LiClO_4$ in PC solvent substantially contributes the conductivity. An examination of Figure 6 reveals that three straight lines with different slopes are obtained for different doping levels of salts. The magnitude of the slope for the three samples is in the order f4 > f3 > f2 for TPU3/$LiClO_4$ series and g4 > g3 > g2 for TPU2/$LiClO_4$ series, respectively. This result implies that the temperature dependence of conductivity for the TPU/$LiClO_4$ gel-type electrolytes (with 50% PC addition) is proportional to the doping level of salt.

It is interesting to note that the magnitude of conductivity for TPU3/$LiClO_4$ series (with 50% PC addition) is approximately similar to that for the TPU2/$LiClO_4$ series at the same doping level of salt. This result reflects the finding that the H-bonding in TPU matrix is completely released with the addition of 50% PC. At a higher temperature, the strength of intermolecular/intermolecular H-bonding is significantly reduced and the mobility energy of molecules (especially for $LiClO_4$ decoupling species) increases. This results in a higher conductivity.

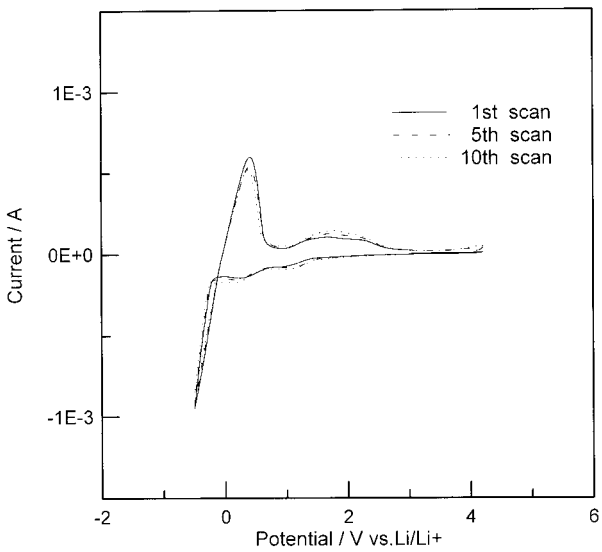

Figure 7 Cyclic voltammogram for the laminated Li/GPE/SS cell.

CV Result

To ascertain the electrochemical stability of the TPU electrolyte, cyclic voltammetry was performed using the three laminated electrode cells at ambient temperature in the grove box. Three representative cyclic voltammograms of sample g4 were presented in Figure 7. The cell was cycled from −0.5 to 4.2 V (versus Li/Li^+) at a sweep rate of 10 mV/s. The cyclic voltammograms are typical of a gel polymer electrolyte. It is evident from Figure 7 that there is no electrochemical reaction in the potential range 1.0 to 4.2 V. The onset of deposition of lithium metal was found at ca. 0.3 V and stripping of lithium metal occurred at ca. 0.5 V. The lithium metal of the plating–stripping process is reversible and there is no other oxidation peak up to 4.2 V. This indicates that TPU electrolytes have good electrochemical stability and can be used as a separator in rechargeable lithium polymer batteries.

CONCLUSION

The soft-segment T_g of TPU samples increases with increasing salt concentration. There are two factors influencing conductivity: one is salt con-

centration, and the other is molecule mobility. There exist interactions between the lithium cation and the electron-rich components (e.g., nitrogen and oxygen) of the urethane moiety via the examination of DSC and FTIR. These interactions are clearly responsible for the result of conductivity. The CV result of the laminated cell using this TPU system as gelled polymer electrolyte shows no electrochemical reaction in the potential range 1.0 to 4.2 V (versus Li/Li^+). In addition, it can also be concluded that the characteristics of PPG-based TPU show suitability for preparing a gelled polymer electrolyte.

The financial support of this work by the National Science Council of the Republic of China under Contract NSC 89-2214-E006-012 is gratefully acknowledged.

REFERENCES

1. Wright, V. Br. Polymer 1975, 7, 319.
2. Armand, M. B. Solid State Ionics 1983 9/10, 745.
3. Gauthier, M.; Belanger, A.; Kapper, B.; Vassort, G.; Armand, M. B. Polymer Electrolytes Review 2; MacCallum, J. R., Vincent, C. A., Eds.; Elsevier: London, 1989; p 285.
4. Anderson, A. M.; Stevens, J. R.; Granqvist, C. G.; Large Area Chromogenics—Materials and Devices for Transmittance Control, Vol. IS4; Lambert, C. M.; Granqvist, C. G., Eds.; Institute Series; Opt. Eng. Press: Bellingham, WA, 1990; p 471.
5. Fauteux, D.; Massucco, A.; Mclin, M.; van Buren, M.; Shi, J. Electrochim Acta 1995, 40, 2185.
6. Ratner, M. A.; Shriver, D. F. Chem Rev 1988, 88, 109.
7. Van Bogart, J. V.; Gibson, P. E.; Cooper, S. L. J Polym Sci, Polym Phys Ed 1983, 21, 65.
8. Koberstein, J. T.; Russell, T. P. Macromolecules 1986, 19, 714.
9. Wang, C. B.; Cooper, S. L. Macromolecules 1983, 16, 775.
10. Yen, M. S.; Kuo, S. C. J Appl Polym Sci 1996, 61, 1639.
11. Seymour, R. W.; Estes, G. M.; Cooper, S. L. Macromolecules 1970, 3, 579.
12. Seefried, C. G.; Koleske, J. V.; Critchfield, F. E. J Appl Polym Sci 1975, 19, 2493.
13. Sung, C. S. P.; Schneider, N. S. Macromolecules 1977, 10, 452.
14. Senich, G. A.; MacKnight, W. J. Macromolecules 1980, 13, 106.
15. Sung, C. S. P.; Hu, C. B. Macromolecules 1981, 14, 212.
16. Brunette, C. M.; Hsu, S. L.; MacKnight, W. J. Macromolecules 1982, 15, 71.
17. Coleman, M. M.; Lee, K. H.; Skrovanek, D. J.; Painter, P. C. Macromolecules 1986, 19, 2149.
18. Lee, H. S.; Wang, Y. K.; Hsu, S. L. Macromolecules 1987, 20, 2089.
19. Pollack, S. K.; Shen, D. Y.; Hsu, S. L.; Wang, Q.; Stidham, H. D. Macromolecules 1989, 22, 551.
20. Zharkov, V. V.; Strikovsky, A. G.; Verteletskaya, T. E. Polymer 1993, 34, 938.
21. Wang, F. C.; Feve, M.; Lam, T. M.; Pascault, J. P. J Polym Sci, Part B: Polym Phys 1994, 32, 1305.
22. Van Heumen, J. D.; Stevens, J. R. Macromolecules 1995, 28, 4268.
23. Wen, T. C.; Wang, Y. J.; Cheng, T. T.; Yang, C. H. Polymer 1999, 40, 3979.
24. Shengqing, X.; Bin, C.; Tao, T.; Baotang, H. Polymer 1999, 40, 3399.
25. Hesketh, T. R.; Van Bogant, Jr., W. C.; Cooper, S. L. Polym Eng Sci 1980, 20, 190.
26. Watanabe, M.; Ohash, S.; Sanui, K.; Ogata, N.; Kobayashi, T.; Ohtaki, E. Macromolecules 1985, 18, 1945.
27. Koberstein, J. T.; Galambos, A. F. Macromolecules 1992, 25, 5618.
28. Seki, M.; Sato, K. Macromol Chem 1992, 93, 2971.
29. McLennaghan, A. W.; Pethrick, R.A. Eur Polym J 1988, 24, 1063.
30. McLennaghan, A. W.; Hooper, A.; Pethrick, R. A. Eur Polym J 1989, 25, 1297.
31. Wen, T. C.; Wu, M. S.; Yang, C. H. Macromolecules 1999, 32, 2712.
32. Moacanin, J.; Cuddihy, E. F. J Polym Sci, Part C 1966, 14, 313.
33. Lu, X.; Weiss, R. A. Macromolecules 1991, 24, 4381.